

Effect of Parameter Mismatch on Partial Synchronization in Coupled Chaotic Systems

Woochang LIM* and Sang-Yoon KIM†

Department of Physics, Kangwon National University, Chunchon 200-701

We investigate the effect of parameter mismatch on partial synchronization in three coupled one-dimensional maps. A completely synchronized attractor on the diagonal loses its transverse stability through a blowout bifurcation, and then partial synchronization may occur on an invariant plane. Due to the existence of positive local transverse Lyapunov exponents, the partially synchronized attractor becomes sensitive with respect to the variation of the mismatching parameter. Thus, in the presence of parameter mismatch, the invariant plane on which partial synchronization occurs is destroyed, and then an intermittent bursting from this plane occurs. To measure the degree of such parameter sensitivity, we introduce the parameter sensitivity exponent and characterize the parameter-mismatching effect on the intermittent bursting. The scaling exponent for the average interburst time is thus found to be given by the reciprocal of the parameter sensitivity exponent.

PACS numbers: 05.45.Xt

Keywords: Partial synchronization, Parameter mismatch

I. INTRODUCTION

Recently, because of its potential practical application (*e.g.*, see [1]), synchronization in coupled chaotic systems has become a field of intensive research. For a sufficiently strong coupling, a complete synchronization where all subsystems become synchronized occurs [2–5]. However, as the coupling parameter decreases and passes a threshold value, the fully synchronized attractor becomes transversely unstable [6–10]. After the breakdown of complete synchronization, partial synchronization where some of the subsystems synchronize while others do not, or complete desynchronization may occur *via* a blowout bifurcation for three or more coupled systems [11–16]. Here, we are interested in the partial synchronization (or clustering) which has been extensively studied in globally coupled systems where each subsystem is coupled to all the other ones with equal strength [17–19].

In a real situation, a small mismatch between the subsystems that destroys the invariant subspace on which partial synchronization occurs is unavoidable. Hence, the effect of the parameter mismatch must be taken into consideration for the study on the partial synchronization. In the regime of partial synchronization, a typical trajectory may have segments exhibiting positive local (finite-time) transverse Lyapunov exponents because of local repulsion of transversely unstable orbits embedded in the partially synchronized attractor. For this case, any small mismatch results in a permanent intermit-

tent bursting. This attractor bubbling demonstrates the sensitivity of the partially synchronized attractor with respect to the variation of the mismatching parameter. Recently, we have introduced a quantifier, called the parameter sensitivity exponent, to measure the degree of the parameter sensitivity of a completely synchronized attractor [20]. Here, we extend the method of quantitatively characterizing the parameter sensitivity to the case of a partially synchronized attractor, and study the parameter-mismatching effect on partial synchronization in terms of the parameter sensitivity exponents.

This paper is organized as follows. In Section II, we introduce the parameter sensitivity exponent for the case of partial synchronization in three coupled one-dimensional (1D) maps, and quantitatively measure the degree of the parameter sensitivity of the partially synchronized attractor by varying the coupling parameter. In terms of these parameter sensitivity exponents, the effect of parameter mismatch on the attractor bubbling (occurring in the regime of partial synchronization) is characterized. Thus, the scaling exponent for the average interburst time is found to be given by the reciprocal of the parameter sensitivity exponent. Finally, we give a summary in Section III.

II. CHARACTERIZATION OF THE PARAMETER-MISMATCHING EFFECT ON PARTIAL SYNCHRONIZATION

We investigate the effect of parameter mismatch on partial synchronization in three coupled 1D maps with a

*E-mail: wclim@kangwon.ac.kr;

†Corresponding Author: sykim@kangwon.ac.kr

parameter tuning the asymmetry in the coupling,

$$x_{n+1}^{(i)} = f(x_n^{(i)}, a_i) + c \left[\sum_{j=1}^3 p_j f(x_n^{(j)}, a_j) - f(x_n^{(i)}, a_i) \right],$$

$$i = 1, 2, 3, \quad (1)$$

where $x_n^{(i)}$ is a state variable of the i th element at a discrete time n , the uncoupled dynamics ($c = 0$) is governed by the 1D map $f(x^{(i)}, a_i) = 1 - a_i x^{(i)2}$ with a control parameter a_i , c is a coupling parameter, and p_j denotes the coupling weight for the j th element ($\sum_{j=1}^3 p_j = 1$). Here, the asymmetric coupling naturally appears when studying the three-cluster dynamics in an ensemble of N globally coupled 1D maps [17–19], where each 1D map is coupled to all the other ones with equal strength. For the case of three clusters with N_j elements in each j th cluster ($j = 1, 2, 3$), $p_j (= N_j/N)$ represents the fraction of the total population of elements in the j th cluster. For the case of unidirectional coupling with $p_2 = p_3 = 0$ (*i.e.*, $p_1 = 1$), the first drive subsystem with the state variable $x^{(1)}$ acts on the second and third response subsystems with the state variables $x^{(2)}$ and $x^{(3)}$, and partial synchronization was observed to occur on an invariant plane *via* a supercritical blowout bifurcation of the fully synchronized attractor on the diagonal [11]. On the other hand, a completely desynchronized 3D attractor appears through the supercritical blowout bifurcation for the case of symmetric coupling with $p_1 = p_2 = p_3 = 1/3$ [16]. We connect these two extreme cases through a path with $p_2 = p_3 \equiv p$ ($0 \leq p \leq 1/3$) in the $p_2 - p_3$ plane and then the parameter p tunes the degree of asymmetry in the coupling of Eq. (1) from the unidirectional coupling ($p = 0$) to the symmetric coupling ($p = 1/3$).

By varying the parameters p and c for the identical case of $a_1 = a_2 = a_3 = 1.95$, we have studied whether an asynchronous attractor born *via* a supercritical blowout bifurcation of the fully synchronized attractor is partially synchronized or completely desynchronized [21]. The completely synchronized attractor lies on the diagonal in the hatched region with horizontal lines in Figure 1(a). As the coupling parameter c decreases and passes a threshold value c_1^* ($\simeq 0.4398$), it becomes transversely unstable, and then partial synchronization (complete desynchronization) occurs for $p < p^*$ ($p > p^*$) ($p^* \simeq 0.146$) in the gray (white) region in Figure 1(a). We note that the partially synchronized attractor exists in the largest interval of the coupling parameter c for the unidirectionally coupled case of $p = 0$.

As an example, we choose the unidirectionally coupled 1D maps,

$$\begin{aligned} x_{n+1}^{(1)} &= f(x_n^{(1)}, a_1), \\ x_{n+1}^{(2)} &= f(x_n^{(2)}, a_2) + c [f(x_n^{(1)}, a_1) - f(x_n^{(2)}, a_2)], \\ x_{n+1}^{(3)} &= f(x_n^{(3)}, a_3) + c [f(x_n^{(1)}, a_1) - f(x_n^{(3)}, a_3)], \end{aligned} \quad (2)$$

where $a_1 = a$, $a_2 = a - \varepsilon_2$, and $a_3 = a - \varepsilon_3$. Here, we fix the value of a as $a = 1.95$ and investigate the

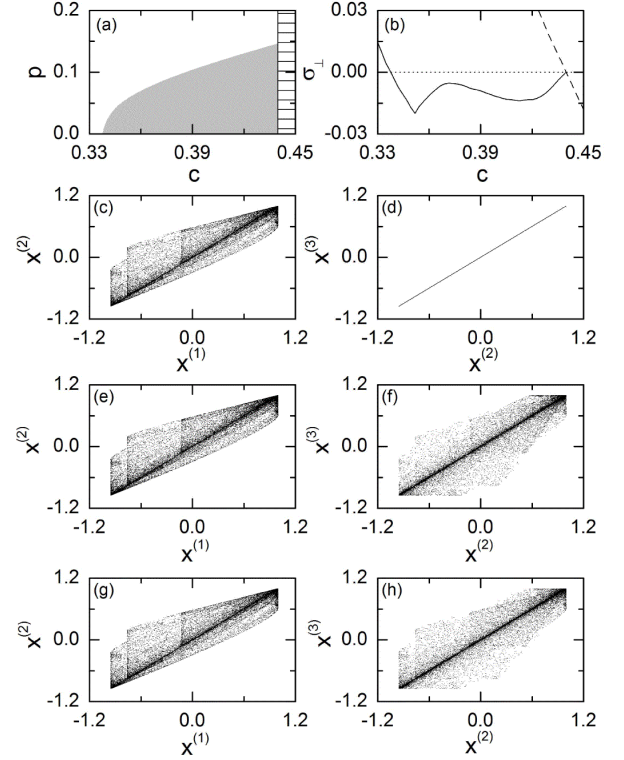


Fig. 1. Effect of parameter mismatch on partial synchronization for $a = 1.95$. (a)-(d) correspond to the ideal case without parameter mismatch. (a) State diagram in the $c - p$ plane. A fully synchronized attractor exists in the hatched region, while a partially synchronized and a completely desynchronized attractor exist in the gray and white regions, respectively. (b) Plot of the transverse Lyapunov exponent of the partially synchronized attractor (denoted by a solid curve) *versus* c in the unidirectionally-coupled case with $p = 0$. The transverse Lyapunov exponent of the fully synchronized attractor is also represented by a dashed line. Projections of a partially synchronized attractor onto the (c) $x^{(1)}-x^{(2)}$ and (d) $x^{(2)}-x^{(3)}$ planes are given for $c = 0.42$. In the presence of parameter mismatch, such a partially synchronized attractor is transformed into a bubbling attractor. (e)-(f) correspond to the mismatching case of $\varepsilon_2 = 0.001$ and $\varepsilon_3 = 0$. Projections of the bubbling attractor onto the (e) $x^{(1)}-x^{(2)}$ and (f) $x^{(2)}-x^{(3)}$ planes are shown for $c = 0.42$. (g)-(h) correspond to the mismatching case of $\varepsilon_2 = 0$ and $\varepsilon_3 = 0.001$. Projections of the bubbling attractor onto the (e) $x^{(1)}-x^{(2)}$ and (f) $x^{(2)}-x^{(3)}$ planes are given for $c = 0.42$.

parameter-mismatching effect on partial synchronization by varying the coupling parameter c . In the ideal case without parameter mismatching (*i.e.*, $\varepsilon_2 = \varepsilon_3 = 0$) a fully synchronized attractor, whose transverse Lyapunov exponent is denoted by a dashed line in Figure 1(b), exists on the invariant diagonal for a sufficiently strong coupling. However, as c decreases and passes a threshold value c_1^* ($\simeq 0.4398$), it loses its transverse stability. Then, a partially synchronized attractor appears *via* a supercritical blowout bifurcation on the invariant Π_{23}

$[= \{(x^{(1)}, x^{(2)}, x^{(3)}) | x^{(2)} = x^{(3)}\}]$ plane, as shown in Figure 1(c) and 1(d) for $c = 0.42$. This partially synchronized attractor satisfies $x_n^{(1)} \equiv X_n$ and $x_n^{(2)} = x_n^{(3)} \equiv Y_n$, and its dynamics is governed by a reduced 2D map,

$$X_{n+1} = f(X_n), \quad Y_{n+1} = f(Y_n) + c[f(X_n) - f(Y_n)]. \quad (3)$$

The transverse Lyapunov exponent σ_{\perp} of the partially synchronized attractor is represented by the solid curve in Figure 1(b). It is transversely stable in the interval of $c_2^*(= 0.3376) < c < c_1^*$ because $\sigma_{\perp} < 0$. As c is decreased from c_1^* , σ_{\perp} begins to increase from $c \simeq 0.413$ after its first decrease. However, it has a decreasing part for $0.372 > c > 0.351$, and then increases to zero for $c \simeq 0.3376$. In the decreasing part, the partially synchronized attractor becomes more transversely stable as c is decreased.

For the case of partial synchronization, there are transversely unstable orbits embedded in the partially synchronized attractor. Due to local transverse repulsion of such unstable orbits, the partially synchronized attractor exhibits a parameter sensitivity. Hence, any small parameter mismatch results in persistent intermittent bursting from the Π_{23} plane, called attractor bubbling. Figure 1(e)-(f) and 1(g)-(h) show such attractor bubbling for both cases of (1) $\varepsilon_2 = 0.001$ and $\varepsilon_3 = 0$, and (2) $\varepsilon_2 = 0$ and $\varepsilon_3 = 0.001$. We first consider the mismatching case between the first and second subsystems (*i.e.*, $\varepsilon_2 \neq 0$ and $\varepsilon_3 = 0$). For this case, the sensitivity of the partially synchronized attractor with respect to the parameter mismatching may be characterized by differentiating the transverse variable $u_n \equiv x_n^{(2)} - x_n^{(3)}$, denoting the deviation from the Π_{23} plane, with respect to ε_2 :

$$\left. \frac{\partial u_{n+1}}{\partial \varepsilon_2} \right|_{\varepsilon_2=0} = \left. \frac{\partial x_{n+1}^{(2)}}{\partial \varepsilon_2} \right|_{\varepsilon_2=0} - \left. \frac{\partial x_{n+1}^{(3)}}{\partial \varepsilon_2} \right|_{\varepsilon_2=0}. \quad (4)$$

Using Eq. (2) we obtain the recurrence relation

$$\left. \frac{\partial u_{n+1}}{\partial \varepsilon_2} \right|_{\varepsilon_2=0} = r(Y_n) \left. \frac{\partial u_n}{\partial \varepsilon_2} \right|_{\varepsilon_2=0} + (c-1)f_a(Y_n, a), \quad (5)$$

where

$$r(Y_n) \equiv (1-c)f_Y(Y_n, a), \quad (6)$$

and f_a and f_Y are the derivatives of f with respect to a and Y , respectively. Iterating the formula (5) along a trajectory starting from an initial orbit point (X_0, Y_0) on the Π_{23} plane, we may obtain derivatives at all subsequent orbit points:

$$\begin{aligned} \left. \frac{\partial u_N}{\partial \varepsilon_2} \right|_{\varepsilon_2=0} &= (c-1) \sum_{k=1}^N R_{N-k}(X_k, Y_k) f_a(Y_{k-1}, a) \\ &+ R_N(X_0, Y_0) \left. \frac{\partial u_0}{\partial \varepsilon_2} \right|_{\varepsilon_2=0}, \end{aligned} \quad (7)$$

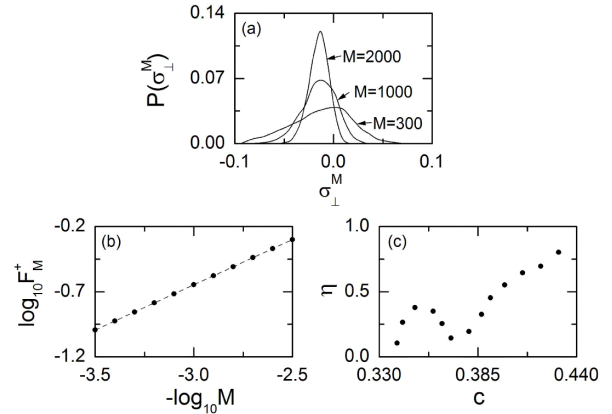


Fig. 2. (a) Three probability distributions $P(\sigma_{\perp}^M)$ of the local M -time Lyapunov exponents for $M = 300, 1000$, and 2000 when $a = 1.95$ and $c = 0.42$. (b) Plot of $\log_{10} F_M^+$ (F_M^+ : fraction of the positive local transverse Lyapunov exponent) versus $-\log_{10} M$ for $c = 0.42$. Note that it is well fitted with the straight line with the slope $\eta = 0.695$. Hence F_M^+ decays with some power η . (c) Plots of η versus c .

where

$$R_M(X_m, Y_m) \equiv \prod_{i=0}^{M-1} r(Y_{m+i}) \quad (M \geq 1) \text{ and } R_0 = 1. \quad (8)$$

Here, the factor $R_M(X_m, Y_m)$ is associated with a local M -time transverse Lyapunov exponent $\sigma_{\perp}^M(X_m, Y_m)$ of the partially synchronized attractor that is averaged over M orbit points starting from (X_m, Y_m) :

$$\begin{aligned} \sigma_{\perp}^M(X_m, Y_m) &= \frac{1}{M} \ln |R_M(X_m, Y_m)| \\ &= \ln |1-c| + \frac{1}{M} \sum_{t=1}^M \ln |f_Y(Y_n, a)|. \end{aligned} \quad (9)$$

Hence, $R_M(X_m, Y_m)$ becomes a local (transverse stability) multiplier determining local sensitivity of the transverse motion during a finite time M . Because the initial point starts on the Π_{23} plane (*i.e.*, $x_0^{(2)} = x_0^{(3)}$), the value of the initial transverse variable $u_0 = x_0^{(2)} - x_0^{(3)}$ is always zero, independently of ε_2 (*i.e.*, $\left. \frac{\partial u_0}{\partial \varepsilon_2} \right|_{\varepsilon_2=0} = 0$). Hence, Eq. (7) is reduced to

$$\begin{aligned} \left. \frac{\partial u_N}{\partial \varepsilon_2} \right|_{\varepsilon_2=0} &= S_N(X_0, Y_0) \\ &\equiv (c-1) \sum_{k=1}^N R_{N-k}(X_k, Y_k) f_a(Y_{k-1}, a). \end{aligned} \quad (10)$$

In the case of partial synchronization, there are transversely unstable periodic orbits embedded in the partially synchronized attractor. When a typical trajectory visits neighborhoods of such transversely unstable periodic orbits, it has segments experiencing local transverse

repulsion from the Π_{23} plane. Thus the distribution of local transverse Lyapunov exponents σ_{\perp}^M for a large ensemble of trajectories and large M may have a positive tail. As an example, we consider the case of $a = 1.95$ and $c = 0.42$ and obtain the probability distribution $P(\sigma_{\perp}^M)$ of local (M -time) transverse Lyapunov exponents, where $P(\sigma_{\perp}^M) d\sigma_{\perp}^M$ is the probability that σ_{\perp}^M has a value between σ_{\perp}^M and $\sigma_{\perp}^M + d\sigma_{\perp}^M$, by taking a long trajectory dividing it into segments of length M , and calculating σ_{\perp}^M in each segment. Figure 2(a) shows the distributions $P(\sigma_{\perp}^M)$ for $M = 300, 1000,$ and 2000 . In the limit $M \rightarrow \infty$, $P(\sigma_{\perp}^M)$ approaches the delta distribution $\delta(\sigma_{\perp}^M - \sigma_{\perp})$, where $\sigma_{\perp} (= -0.0135)$ is the usual averaged transverse Lyapunov exponent. However, we note that the distribution $P(\sigma_{\perp}^M)$ has a significant positive tail which does not vanish even for large M . To quantify this slow decay of the positive tail, we define the fraction of positive local transverse Lyapunov exponents as

$$F_M^+ = \int_0^{\infty} P(\sigma_{\perp}^M) d\sigma_{\perp}^M. \quad (11)$$

This fraction F_M^+ is plotted for $c = 0.42$ in Figure 2(b), and it exhibits a power-law decay with the exponent $\eta = 0.695$,

$$F_M^+ \sim M^{-\eta}. \quad (12)$$

By decreasing the coupling parameter c from c_1^* , we obtain the exponents η which are shown in Figure 2(c). Consequently, for any case of partial synchronization, a trajectory has segments of arbitrarily long M that have positive local Lyapunov exponents. Then, the local multipliers $R_M [= \pm \exp(\sigma_{\perp}^M M)]$ can be arbitrarily large, and hence the partial sum S_N of Eq. (10) may be arbitrarily large. This implies unbounded growth of the derivatives $\left. \frac{\partial u_N}{\partial \varepsilon} \right|_{\varepsilon=0}$ as N tends to infinity, and consequently the partially synchronized attractor exhibits a parameter sensitivity. As c is decreased from c_1^* , the value of F_M^+ becomes larger because the exponent η is smaller. Hence, the degree of parameter sensitivity increases. However, in the decreasing part of σ_{\perp} ($0.372 > c > 0.351$) [see Figure 1(b)], the value of η increases, and hence the degree of parameter sensitivity becomes weaker in this interval. For $c < 0.351$, the value of η begins to decrease again, which results in the increase in the degree of parameter sensitivity.

As an example, we consider the partially synchronized attractor for $c = 0.42$ [see Figure 1(c) and (d)]. To quantitatively characterize its parameter sensitivity, we iterate Eqs. (3) and (5) starting from an initial orbit point (X_0, Y_0) on the Π_{23} plane and $\left. \frac{\partial u_0}{\partial \varepsilon} \right|_{\varepsilon_2=0} = 0$, and then we obtain the partial sum $S_N(X_0, Y_0)$ of Eq. (10). The quantity S_N becomes very intermittent. However, looking only at the maximum

$$\gamma_N(X_0, Y_0) = \max_{0 \leq n \leq N} |S_n(X_0, Y_0)|, \quad (13)$$

one can easily see the boundedness of S_N . Note that $\gamma_N(X_0, Y_0)$ depends on a particular trajectory. To obtain a representative quantity, we consider an ensemble

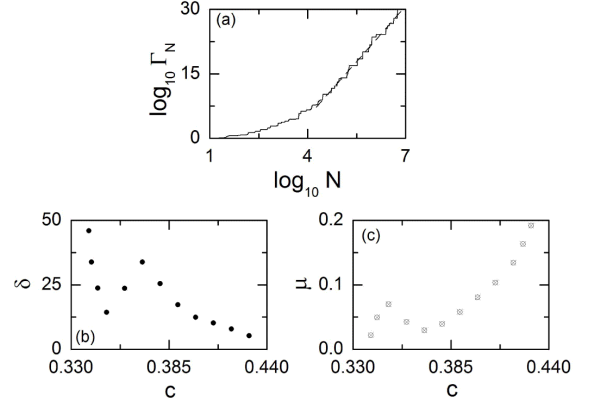


Fig. 3. (a) Parameter sensitivity function Γ_N for $a = 1.95$ and $c = 0.42$. The data are well fitted with a straight line (represented by a dashed line) with slope $\delta = 7.915$. (b) Plot of the parameter sensitivity exponents δ versus c . (c) Plot of the scaling exponents μ (open circles) versus c . They agree well with the reciprocals of the parameter sensitivity exponents (crosses).

of randomly chosen initial points $\{(X_0, Y_0)\}$ on the Π_{23} plane and then take the minimum value of $\gamma_N(X_0, Y_0)$ with respect to the initial orbit points,

$$\Gamma_N = \min_{\{(X_0, Y_0)\}} \gamma_N(X_0, Y_0). \quad (14)$$

For the case of partial synchronization, the parameter sensitivity function Γ_N grows unboundedly with some power δ ,

$$\Gamma_N \sim N^\delta, \quad (15)$$

as shown in Figure 3(a). Here, $\delta (= 7.915)$ is a quantitative characteristic of the parameter sensitivity of the partially synchronized attractor, and we call it the parameter sensitivity exponent. By decreasing the coupling parameter c from c_1^* , we obtain the parameter sensitivity exponents. For obtaining satisfactory statistics, we consider 100 ensembles for each c , each of which contains 100 initial orbit points randomly chosen with uniform probability in the square with side of length 0.5 centered at $(X, Y) = (0.25, 0.25)$ on the Π_{23} plane and choose the average value of the 100 parameter sensitivity exponents obtained in the 100 ensembles. Figure 3(b) shows a plot of such parameter sensitivity exponents versus c . As c is decreased from c_1^* , the parameter sensitivity exponent δ increases because of the increase in the strength of local transverse repulsion of unstable orbits embedded in the partially synchronized attractor. However, in the decreasing part of σ_{\perp} ($0.372 > c > 0.351$) the value of δ becomes smaller, since the strength of local transverse repulsion of unstable orbits becomes weaker. For $c < 0.351$, δ begins to increase again.

Because of its sensitivity with respect to the variation of ε_2 , the partially synchronized attractor transforms into a bubbling attractor [e.g., see Figure 1(e)

and (f)]. We characterize the parameter-mismatching effect on the attractor bubbling in terms of the parameter sensitivity exponents. The bubbling attractor is in the laminar phase when the magnitude of the deviation $d [\equiv |u|(= |x^{(2)} - x^{(3)}|)]$ from the Π_{23} plane is less than a threshold value d^* . Otherwise, it is in the bursting phase. For this case, the quantity of interest is the average time τ that a typical trajectory spends near the Π_{23} plane. For each c , we follow the trajectory starting from the initial condition $(x^{(1)}, x^{(2)}, x^{(3)}) = (0.26, 0.25, 0.25)$ until 50,000 laminar phases are obtained, and then we get the average laminar length τ (*i.e.*, the average interburst interval) that scales with ε_2 as

$$\tau \sim \varepsilon_2^{-\mu}. \quad (16)$$

The plot of μ (open circles) *versus* c is shown in Figure 3(c). As c is decreased from c_1^* , the value of μ decreases, because the average laminar length shortens. However, in the decreasing part of σ_{\perp} ($0.372 > c > 0.351$) the average laminar length τ becomes longer, and hence the value of μ becomes larger. For $c < 0.351$, μ begins to decrease again. We note that the scaling exponent μ is associated with the parameter sensitivity exponent δ as follows. For a given ε_2 , consider a trajectory starting from a randomly chosen initial orbit point on the Π_{23} plane. Then, from Eq. (14) the ‘‘average’’ time τ at which the magnitude of the deviation from the Π_{23} plane becomes the threshold value d^* can be obtained:

$$\tau \sim \varepsilon_2^{-1/\delta}. \quad (17)$$

Thus, the two exponents have a reciprocal relation,

$$\mu = 1/\delta. \quad (18)$$

The reciprocal values of δ (crosses) are also plotted in Figure 3(c), and they agree well with the values of μ .

So far, we have studied the mismatching case between the first and second subsystems. We now compare the formula (10) for the partial sum S_N with the following analogous formula for S_N that is obtained in the mismatching case between the first and third case (*i.e.*, $\varepsilon_3 \neq 0$ and $\varepsilon_2 = 0$),

$$\begin{aligned} \left. \frac{\partial u_N}{\partial \varepsilon_3} \right|_{\varepsilon_3=0} &= S_N(X_0, Y_0) \\ &\equiv (1-c) \sum_{k=1}^N R_{N-k}(X_k, Y_k) f_a(Y_{k-1}, a). \end{aligned} \quad (19)$$

For both cases, S_N represents the sum of the (same) local multipliers R_{N-k} , multiplied by some coefficients $[(c-1)f_a$ for Eq. (10) and $(1-c)f_a$ for Eq. (19)]. Since the values of f_a are bounded in the interval $[-1, 0]$, the boundedness of S_N is determined only by the (same) local multipliers R_M for both cases. This implies that the parameter sensitivity function Γ_N for the case of $\varepsilon_3 \neq 0$ grows unboundedly with the same power as in the above case of $\varepsilon_2 \neq 0$. Consequently, we have the same parameter sensitivity exponent δ for both cases.

III. SUMMARY

We have studied the effect of parameter mismatch on partial synchronization in three coupled 1D maps. Due to the existence of positive local transverse Lyapunov exponents, the partially synchronized attractor has a parameter sensitivity. To measure the degree of such parameter sensitivity, we have introduced the parameter sensitivity exponent and quantitatively characterized the parameter-mismatching effect on attractor bubbling occurring in the regime of partial synchronization. It has thus been found that the scaling exponent μ for the average interburst time and the parameter sensitivity exponent δ have a reciprocal relation (*i.e.*, $\mu = 1/\delta$).

ACKNOWLEDGMENTS

This work was supported by the Korea Research Foundation (Grant No. R05-2004-000-10717-0).

REFERENCES

- [1] K. M. Cuomo and A. V. Oppenheim, Phys. Rev. Lett. **71**, 65 (1993); L. Kocarev, K. S. Halle, K. Eckert, L. O. Chua and U. Parlitz, Int. J. Bifurcation Chaos Appl. Sci. Eng. **2**, 973 (1992); L. Kocarev and U. Parlitz, Phys. Rev. Lett. **74**, 5028 (1995); N. F. Rulkov, Chaos **6**, 262 (1996).
- [2] H. Fujisaka and T. Yamada, Prog. Theor. Phys. **69**, 32 (1983).
- [3] A. S. Pikovsky, Z. Phys. B: Condens. Matter **50**, 149 (1984).
- [4] V. S. Afraimovich, N. N. Verichev and M. I. Rabinovich, Radiophys. Quantum Electron. **29**, 795 (1986).
- [5] L. M. Pecora and T. L. Carroll, Phys. Rev. Lett. **64**, 821 (1990).
- [6] E. Ott and J. C. Sommerer, Phys. Lett. A **188**, 39 (1994).
- [7] P. Ashwin, P. J. Aston and M. Nicol, Physica D **111**, 81 (1998).
- [8] Y. Nagai and Y.-C. Lai, Phys. Rev. E **55**, R1251 (1997); *ibid* **56**, 4031 (1997).
- [9] P. Glendinning, Phys. Lett. A **264**, 303 (1999).
- [10] S.-Y. Kim, W. Lim, E. Ott and B. Hunt, Phys. Rev. E **68**, 066203 (2003).
- [11] K. Pyragas, Phys. Rev. E **54**, R4508 (1996).
- [12] M. S. Vieira and A. J. Lichtenberg, Phys. Rev. E **56**, R3741 (1997).
- [13] M. Hasler, Yu. Maistrenko and O. Popovych, Phys. Rev. E **58**, 6843 (1998); Yu. Maistrenko, O. Popovych and M. Hasler, Int. J. Bifurcation Chaos Appl. Sci. Eng. **10**, 179 (2000); A. V. Taborov, Yu. Maistrenko and E. Mosekilde, Int. J. Bifurcation Chaos Appl. Sci. Eng. **10**, 1051 (2000); S. Yanchuk, Yu. Maistrenko and E. Mosekilde, Chaos **13**, 388 (2003).
- [14] M. Inoue, T. Kawazoe, Y. Nishi and M. Nagadome, Phys. Lett. A **249**, 69 (1998).

- [15] Y. Zing, G. Hu, H. A. Cerdera, S. Chen, T. Braun and Y. Yao, *Phys. Rev. E* **63**, 026211 (2001).
- [16] N. Tsukamoto, S. Miyazaki and H. Fujisaka, *Phys. Rev. E* **67**, 016212 (2003).
- [17] K. Kaneko, *Physica D* **41**, 137 (1990).
- [18] O. Popovych, Yu. Maistrenko and E. Mosekilde, *Phys. Rev. E* **64**, 026205 (2001).
- [19] O. Popovych, Yu. Maistrenko and E. Mosekilde, *Phys. Lett. A* **302**, 171 (2002).
- [20] A. Jalnine and S.-Y. Kim, *Phys. Rev. E* **65**, 026210 (2002); W. Lim and S.-Y. Kim, *J. Phys. A* **37**, 8233 (2004); W. Lim and S.-Y. Kim, *J. Korean Phys. Soc.* **44**, 510 (2004).
- [21] W. Lim and S.-Y. Kim, *Phys. Rev. E* **71**, 036221 (2005); W. Lim and S.-Y. Kim, *J. Korean Phys. Soc.* **46**, 638 (2005).